# Polymorphism on Leflunomide: Stability and Crystal Structures

DANIEL VEGA,[1,2] ALICIA PETRAGALLI,[1] DANIEL FERNÁNDEZ,[2] JAVIER A. ELLENA[3]

[1]Unidad de Actividad Física, Comisión Nacional de Energía Atómica, Av. Gral. Paz 1499, 1650 San Martín, Buenos Aires, Argentina

[2]Escuela de Ciencia y Tecnología, Universidad Nacional de General San Martín, Calle 91 3391, 1653 Villa Ballester, Buenos Aires, Argentina

[3]Departamento de Física e Informática, Instituto de Física de São Carlos, Universidade de São Paulo, Caixa Postal 369, CEP 13560-970, São Carlos, SP, Brazil

*Received 29 September 2004; revised 8 March 2005; accepted 9 March 2005*

*Published online in Wiley InterScience (www.interscience.wiley.com). DOI 10.1002/jps.20382*

**ABSTRACT:** Two polymorphs of Leflunomide were found and studied (form I and II). Both of them were characterized by X-ray powder diffraction and thermal analysis. Single crystals were obtained and both structures were solved. Forms I and II crystallize in the space group $P2_1/c$ with two and one independent molecules per asymmetric unit, respectively. Thermodynamic stability of the two forms is assessed by differential scanning calorimetry. The cohesion in the crystal of form I (the more stable) is provided by both by H bonding as well as $\pi \ldots \pi$ interactions, while in form II it is given only by the former. The independent molecules in form I adopt different conformations thus allowing for a larger number of intermolecular interactions. © 2006 Wiley-Liss, Inc. and the American Pharmacists Association J Pharm Sci 95:1075–1083, 2006

**Keywords:** crystal structure; polymorphism; thermal analysis; physical stability; calorimetry (DSC); phase transition; crystals; x-ray diffractometry; thermodynamics; x-ray powder diffractometry

## INTRODUCTION

One of the primary goals of crystal engineering[1] is to design and control the way the molecules crystallize, producing materials with specific properties. If crystals of pharmaceuticals could be engineered, then properties such as stability, bioavailability, and processibility could be optimized.[2] For these type of compounds the structure-property relationships are governed only by differences in the spatial arrangement of the constituent molecules in the crystal, and in some cases, by variations in molecular conformation. Pharmaceutical polymorphism[3] can be viewed as part of the crystal engineering area and it allows a safe manipulation of the crystal properties of solids.[4] The importance of polymorphism knowledge increases because of the fact that sometimes the most stable polymorph is difficult to produce, or a metastable form has more favorable properties, so it is of the greatest importance for pharmaceutical industry to ensure reliable and robust processes, accordingly with GMP, considered even today a regulatory requirement.

In the present paper, our main scope is to provide physical information on stability and crystal structures of two polymorphs of Leflunomide (Fig. 1).

Leflunomide is a drug used for the treatment of rheumatoid arthritis, an illness that affects soft tissues and bones and can cause irreversible

*Correspondence to*: Daniel Vega (Telephone: +54 11 6772-7107; Fax: +54 11 6772-7121)

Journal of Pharmaceutical Sciences, Vol. 95, 1075–1083 (2006)

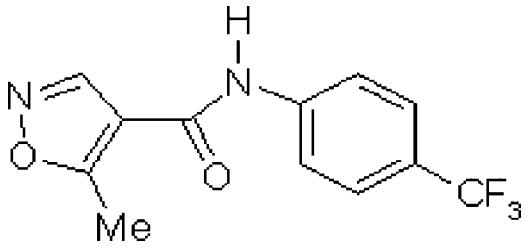


**Figure 1.** Drawing of Leflunomide molecule.

joint deformities and functional impairment. This autoimmune disease is originated by rapidly dividing lymphocytes, which are activated in response to an as yet unknown antigen.[5] Proliferating cells require expanded intracellular pools of uracil, cytosine, and thymine nucleotides; hence, blocking the *de novo* synthesis of pyrimidines is a means to inhibit cell division.[6] The rate-limiting enzyme in this pathway, dihydroorotate dehydrogenase (dihydroorotase) has been shown to be selectively inhibited by the active metabolite of Leflunomide, thus leading to an antiproliferative action.[7,8] In addition, dihydroorotate dehydrogenase inhibitors can be used to treat infections by human pathogens like Plasmodium falciparum, the causative agent of malaria, and Helicobacter pylori, causing duodenal ulcers, and stomach cancer.[9] At variance with other new drugs for the treatment of rheumatoid arthritis, Leflunomide is administered orally,[10] and its bioavailability is 80%.[11] In spite of its rather high bioavailability, Leflunomide is practically insoluble in water (less than 40 mg/L), so belongs to class II of the biopharmaceutics classification systems (BCS) and then studies on polymorphism are essential in this compound.

## EXPERIMENTAL

### Materials

Powdered samples of Leflunomide were generously provided by ARYL SA, Buenos Aires, Argentina. It was recrystallized from ethanol (99.9%) and benzene (99%) to obtain forms I and II respectively dissolving 5 mg of Leflunomide in 10 mL of solvent at room temperature (25(2)°C). Colorless prismatic single crystals were grown by slow evaporation techniques at room temperature and they were found to be suitable for single crystal X-ray diffraction analysis.

### Methods

#### *X-ray Powder Diffraction*

*X-ray Powder Diffraction* (XRPD) patterns were recorded on a X'Pert Philips PW3020 diffractometer (Philips, The Netherlands) over the 2θ range of 5°–40°, using graphite monochromatized Cu $K_\alpha$ radiation (1.54184 Å), in aluminum sample holders, at room temperature (1° divergence slit; 1° detector slit and 0.1 mm receiving slit, scanning step 0.02°, counting time 2 s). Original provided samples were found to be suitable for XRPD measurement, particle size of 5 μm.

#### *Single Crystal X-ray Diffraction*

*Single crystal X-ray diffraction* data were collected at room temperature, using an AFC6S (Rigaku Corporation, Japan) and an Enraf-Nonius CAD-4 (Bruker Nonius B.V., Delft, The Netherlands) diffractometers for form I and II, respectively. Data-collection strategy and data reduction followed standard procedures implemented in the MSC/AFC[12] and CAD-4[13] software.

The structures were solved using program SHELXS-97[14] and refined using the full-matrix LS procedure with SHELXL-97.[14] Anisotropic displacement parameters were employed for nonhydrogen atoms and H atoms were treated isotropically with $U_{iso} = 1.2$ (for those attached to aromatic carbons and to the N atom) or 1.5 times (for those bonded to methyl carbons) the $U_{eq}$ of the parent atoms. All H atoms were located at the expected positions and they were refined using a riding model. In the final cycle of refinement, LS weights of the form $w = 1/[\sigma^2(F_o^2) + (a*P)^2 + b*P]$, where $P = [(F_o^2) + 2* F_c^2)]/3$, were employed. Routines employed to create CIF files are from WinGX package.[15]

Full use of the Cambridge structural database (CSD) at the CCDC[16] was also made for comparison purposes. Crystallographic data (excluding structure factors) for both forms have been deposited with the Cambridge crystallographic data center as supplementary publications No. CCDC 259170 and 259171.

#### *Differential Scanning Calorimetry*

*Differential scanning calorimetry* (DSC) was carried out with a Shimadzu DSC-60 instrument (Shimadzu, Kyoto, Japan). Samples weighing 3–5 mg were heated in opened aluminum pans at a rate of 10 K/min under nitrogen gas flow of 35 mL/min.

 DOI 10.1002/jps

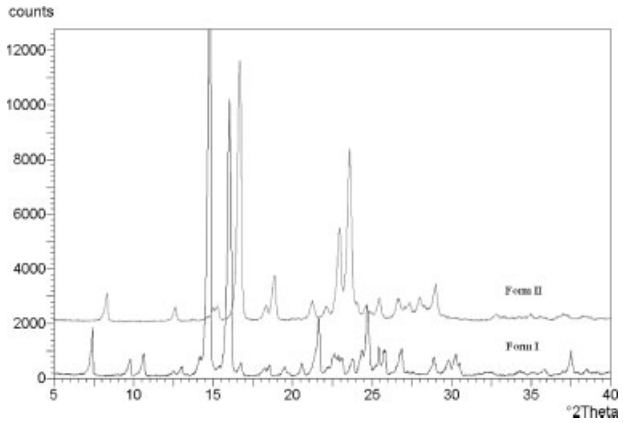


**Figure 2.** X-ray powder diffraction patterns of form I and II.

### *Polarized Thermomicroscopy*

*Polarized thermomicroscopy* was performed using a Kofler hot stage (Thermovar, Reichert, Vienna, Austria) in a Ortholux II POL-BK microscope (Leitz-Wetzlar, Germany).

### *UV-Visible Absorbance*

*UV-Visible absorbance* was measured using a Shimadzu UV-160A spectrophotometer (Shimadzu, Kyoto, Japan) in the range 200–900 nm using a quartz recipient with an optical pathway of 1 cm.

*Saturated water solutions.* Saturated solutions of form I and II were generated by placing an excess amount of sample (7 mg) in 100 mL of water. The suspension was stirred during 24 h at room temperature (25(2)°C) and the final solutions were filtered using 0.2 μm Millipore filter (final measured pH:5). No extra dilution was necessary.

*Saturated ethanol solutions.* Saturated solutions of form I and II were obtained by placing an excess amount of sample (0.1 g) in 0.5 mL of absolute ethanol. The suspension was stirred during 4 h at room temperature in capped glass vials. The solutions were filtered using 0.2 μm Millipore filter and analyzed after appropriate dilution.

**Table 1.** Crystal Data and Refinement Details

| | Form I | Form II |
|---|---|---|
| Chemical formula | $C_{12}H_9F_3N_2O_2$ | |
| Formula weight | 270.21 | |
| Temperature | 293(2) K | |
| Crystal system | Monoclinic | |
| Space group | $P2_1/c$ | |
| Unit cell dimensions | a = 12.345(6) Å | a = 10.578(7) Å |
| | b = 13.813(8) Å | b = 7.9978(9) Å |
| | c = 14.40(2) Å | c = 14.228(2) Å |
| | α = 90.0° | α = 90.0° |
| | β = 103.51(5)° | β = 92.89(4)° |
| | γ = 90.0° | γ = 90.0° |
| Volume | 2388(3) $Å^3$ | 1202.2(8) $Å^3$ |
| Z | 8 | 4 |
| Density (calculated) | 1.503 $g/cm^3$ | 1.493 $g/cm^3$ |
| Radiation, wavelength | MoKα, 0.71073 Å | CuKα, 1.54184 Å |
| Absorption coefficient | 0.135/mm | 1.175/mm |
| F(000) | 1104 | 552 |
| Crystal size | 0.45 × 0.45 × 0.30 mm | 0.225 × 0.2 × 0.125 mm |
| Theta range for data collection | 2.07 to 25.03° | 4.18 to 67.05° |
| Index ranges | $-1 \le h \le 14$, $-16 \le k \le 16$, $-17 \le l \le 16$ | $0 \le h \le 12$, $0 \le k \le 9$, $-16 \le l \le 16$ |
| Reflections collected | 9446 | 2274 |
| Observed reflections ($I > 2\sigma(I)$) | 2633 | 1574 |
| Independent reflections | 4197 | 2151 |
| Internal consistency | $R_{int} = 0.0723$ | $R_{int} = 0.0245$ |
| Refinement method | Full matrix on $F^2$ | |
| Data/restraints/parameters | 4197/0/362 | 2151/0/200 |
| Goodness-of-fit on $F^2$ | 1.027 | 1.058 |
| Final R indices [$I > 2\sigma(I)$] | $R_1 = 0.0439$, $wR^2 = 0.1055$ | $R_1 = 0.0471$, $wR^2 = 0.1297$ |
| R indices (all data) | $R_1 = 0.0867$, $wR^2 = 0.1235$ | $R_1 = 0.0692$, $wR^2 = 0.1437$ |
| Largest difference peak and hole | 0.238, −0.330e/$Å^3$ | 0.236, −0.169e/$Å^3$ |

## RESULTS

### Structure Analysis

The room temperature XRPD patterns of forms I and II are shown in Figure 2. Important differences are clearly visible from this figure.

Single crystal data and refinement details are listed in Table 1, geometrical data is given in Table 2; molecular and packing diagrams are shown in Figures 3–6. Leflunomide crystals belong to the monoclinic crystal system and the space group $P2_1/c$; in form I, there are two independent molecules (labeled A and B) per asymmetric unit, while there is only one in form II (labeled as C). The $CF_3$ groups of molecules A and C were found to be disordered and the fluorine atoms were refined over two positions with refined site-occupation factors in the ratio 0.70:0.30. Leflunomide molecule consists of the 5-methyl isoxazole, amide and trifluoromethylphenyl groups. Bond lengths and angles within these groups are in good agreement between the A, B, and C molecules. Methyl C12 atom is cis with respect to the carbonyl O2 atom and the amide group joining the terminal rings is trans. Molecules A and C are essentially planar with the planes of the isoxazole, amide and phenyl groups sustaining angles less than 8°. In molecule B, the terminal isoxazole and phenyl rings are almost coplanar; however, the amide group deviates from them by ca. 24°. The bond distances between the three groups (C2-C4 and C5-N2) are formal single bonds so that the coplanarity in the A and C molecules could be ascribed to the presence of the intramolecular short contact between the hydrogen atom from the phenyl ring (C10) and the oxygen one from the carbonyl (O2) thus forming a six-membered ring. In molecule B, the C10...O2 intramolecular contact distance is larger because of the rotation

**Table 2.** Selected Geometrical Data (Distances in Å and Angles in °)

| | Form I | | Form II |
|---|---|---|---|
| | A | B | C |
| Overall LS-plane[a] | 0.0528 | 0.1638 | 0.0194 |
| Angles between planes | | | |
| Isoxazole-amide | 5.48(9) | 23.9(1) | 2.2(2) |
| Amide-phenyl | 1.89(9) | 21.4(1) | 1.3(2) |
| Isoxazole-phenyl | 7.12(9) | 6.20(8) | 2.1(2) |
| Bond distances | | | |
| Isoxazole-amide (C2-C4) | 1.482(3) | 1.470(3) | 1.476(3) |
| Amide-phenyl (C5-N2) | 1.408(2) | 1.413(3) | 1.406(3) |
| Intramolecular short contacts[b] | | | |
| C10-O2 | 2.855(4), 122 | 2.868(5), 116 | 2.850(3), 122 |
| Torsion angles | | | |
| C4-C2-C3-C12 | 1.1(4) | 4.5(4) | 0.3(5) |
| C4-N2-C5-C10 | −2.1(3) | −24.8(3) | −0.5(4) |
| C2-C4-N2-C5 | −177.8(2) | −171.9(2) | −178.9(2) |
| Intermolecular hydrogen bonds[c] | | | |
| N2A−H2A...O2B | 2.969(3), 2.13, 164 | | |
| N2B−H2B...N1A[d] | | 3.197(3), 2.35, 170 | |
| N2C−H2C...N1C[e] | | | 3.143(3), 2.36, 151 |
| Angle between planes of molecules connected by the N−H...N Hydrogen bond | | | |
| Isoxazole-amide | | 77.0(1) | 59.81(8) |
| Phenyl-phenyl | | 84.2(1) | 57.12(7) |
| Isoxazole-isoxazole | | 85.9(1) | 60.87(8) |
| Amide-amide | | 82.1(1) | 58.68(8) |

[a] LS-plane through C, N and O atoms (H and F atoms omitted); the r.m.s. deviation of the fitted atoms is given.
[b] Donor-acceptor distance and angle.
[c] Donor and acceptor atoms distances and angle are: DA, HA and D−HA.
[d] Symmetry code: $-x+2, y+0.5, -z+0.5$.
[e] Symmetry code: $-x+1, y-0.5, -z+0.5$.

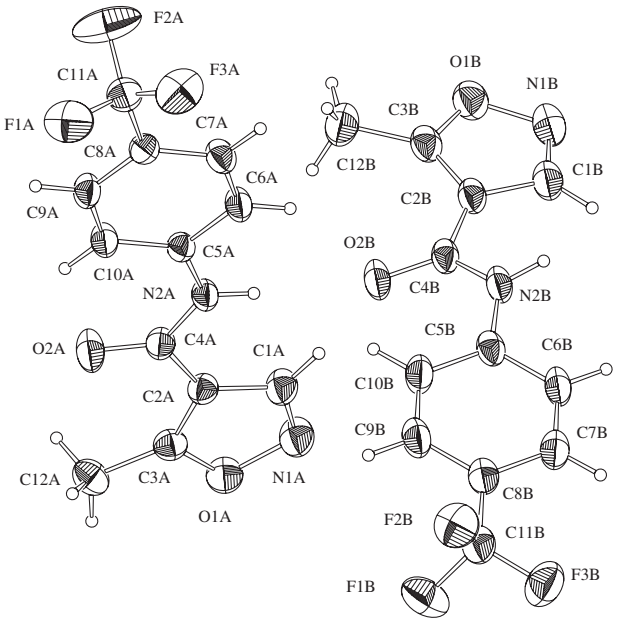


**Figure 3.** ZORTEP[20] representation of independent molecules A and B of Leflunomide Form I showing the numbering scheme used and displacement ellipsoids drawn at the 30% probability level (only the F atoms of the major occupancy component are shown).

of the amide group. Nevertheless, molecules B are able of having $\pi \ldots \pi$ interactions between O1B-N1B-C1B-C2B-C3B cycle and a symmetrically related C5B-C6B-C7B-C8B-C9B-C10B cycle, with a center–center distance of 3.83 Å and a slippage angle of 30°, providing an extra cohesion to the packing of form I. A and B molecules in form I form a chain which is parallel to the crystallographic b axis through N2B–H2B ... N1A and N2A–H2A ... O2B hydrogen bonds, both of them involving the amide group from molecule B. A different arrangement of molecules is found for form II where the molecules interact only via the N2C–H2C ... N1C hydrogen bond. The hydrogen bond between amide and isoxazole groups, has comparable geometric features in both forms except for the donor-H ... acceptor atom angle. The mutual orientation of the planes of molecules connected by the N–H ... N hydrogen bond is roughly 90° for form I molecules, while this relationship is ~25° less for form II thus explaining the difference of the N–H ... N angle.

## Thermal Studies

The DSC trace of form I and II are shown in Figure 7. Both diagrams show endothermal peaks, none of which is related to weight loss as checked

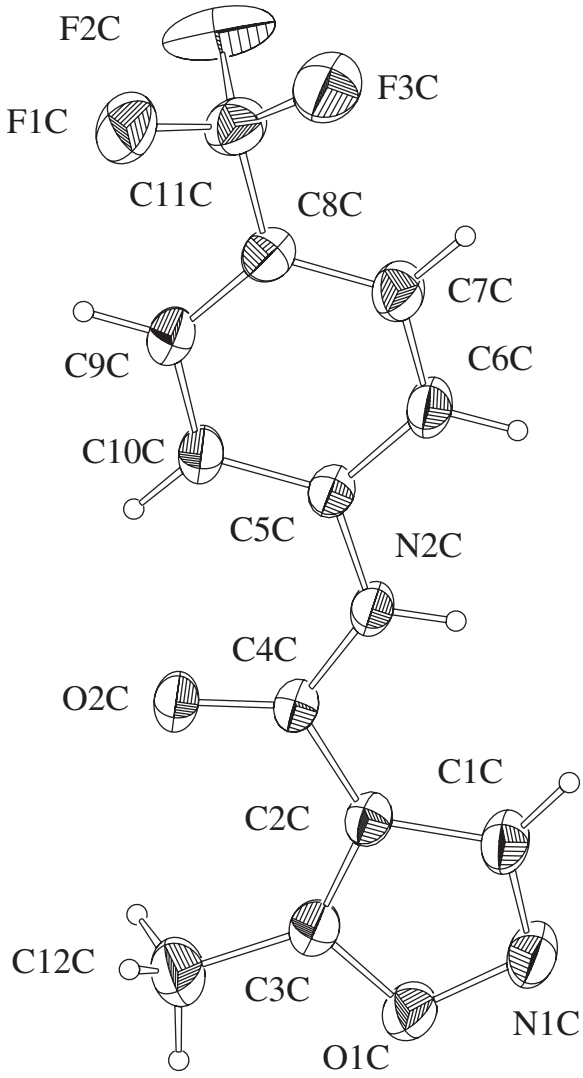


**Figure 4.** ZORTEP[20] representation of molecule C of Leflunomide Form II showing the numbering scheme used and displacement ellipsoids drawn at the 30% probability level (only the F atoms of the major occupancy component are shown).

by TG analysis. In both cases the transition with $T_{onset}$ at about 165°C was observed by visual inspection under polarized thermomicroscopy and is related to the melting of the sample, with an enthalpy difference of about 120 J/g. For form II this is the only event in the thermal behavior; form I shows instead an extra endothermal peak with $T_{onset}$ at about 127°C, involving an enthalpy change of about 18 J/g. By cycling the samples between room temperature and T = 150°C no signs of reversibility could be observed.

Visual inspection with a polarized thermomicroscopy showed that form I exhibit a solid state phase transition before melting, when the first

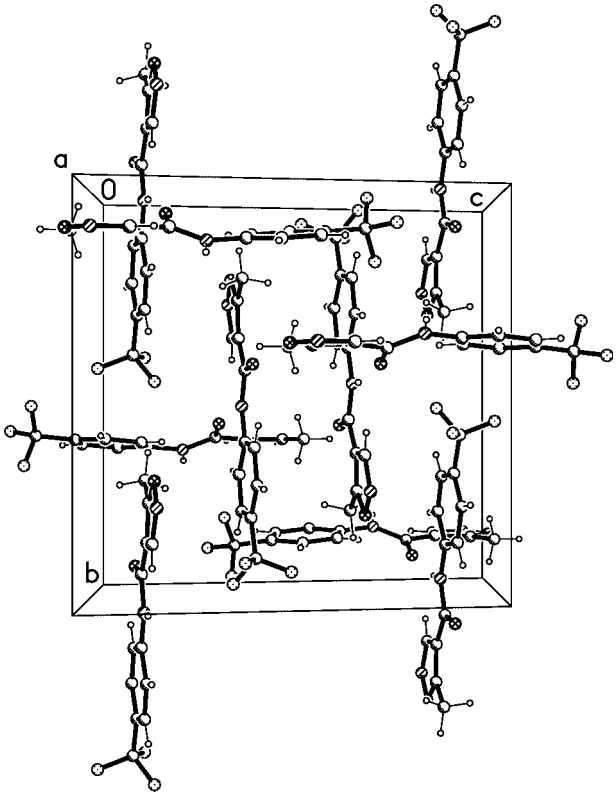


**Figure 5.** Packing diagram of Leflunomide Form I.

endotherm appears (about 127°C). Figure 8 shows some crystals of form I before the transition (top-left), during transition (top-right and bottom-left), and after transition (bottom-right). When the transition begins part of the crystal changes its optical properties and a zone of different color can

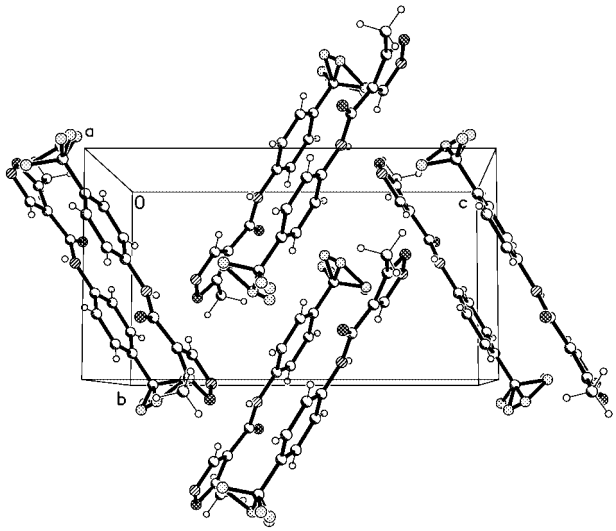


**Figure 6.** Packing diagram of Leflunomide Form II.

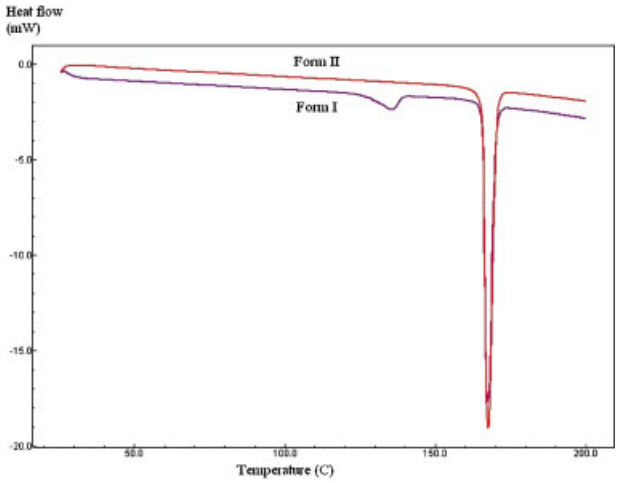


**Figure 7.** Differential scanning calorimetry (DSC) of form I and II.

be observed (see Fig. 8 top-right). The transition continues and the zone advances (see Fig. 8 bottom-left) until the crystal transforms completely (see Fig. 8 bottom-right). Besides, some crystals jump from the sample holder when the transition takes place (see Fig. 8).

### UV-Visible Absorbance Studies

Absorbance spectra for solutions of form I and II in water and ethanol are shown in Figures 9

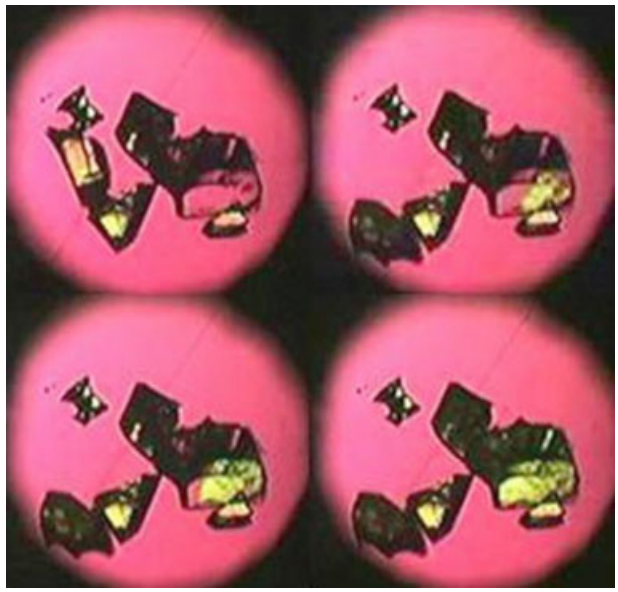

**Figure 8.** Thermomicroscopy of crystals of form I before the transition (top-left), when the transition started (top-right), the transition advances (bottom-left), and after transition (bottom-right).

 DOI 10.1002/jps

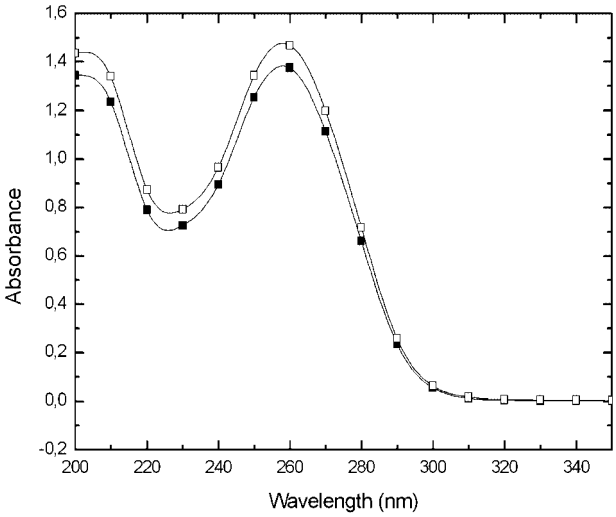


**Figure 9.** Absorbance of water solution of form I (closed squares) and form II (open squares).

and 10, respectively in the range 200–350 nm. Two maxima were observed at 200 and 260 nm (see Fig. 9) and 210 and 260 nm (see Fig. 10) for water and ethanol, respectively. These maxima correspond to two different electronic transitions indicating that two different conformations are present in the equilibrium solutions. The absorbance traces for both forms in the same solvent match perfectly when a normalization factor of 1.07 is applied (form II = 1.07 *form I).

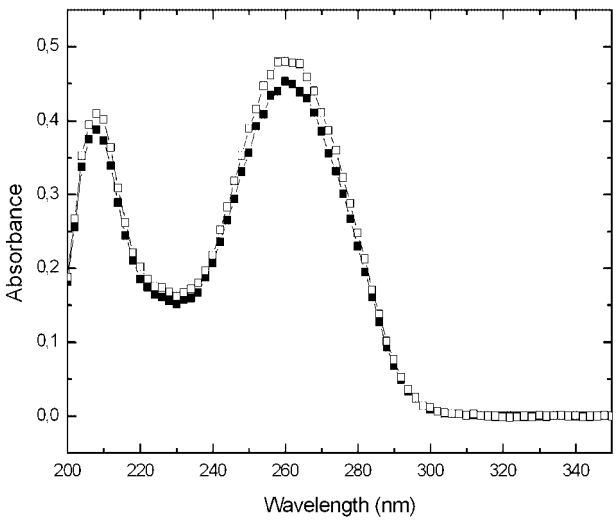


**Figure 10.** Absorbance of ethanol solution of form I (closed squares) and form II (open squares).

## DISCUSSION

Due to the fact that form I suffers a solid-state phase transition, it was possible to quench a sample of form I after transformation and investigate it by XRPD. As the result of this experiment, an unambiguous form II XRPD diagram was observed, indicating that the first endotherm corresponds to transformation of form I to form II and the enthalpy difference correspond to $\Delta H_{I\text{-}II}$:18 J/g. After the transformation takes place, form II melts and the corresponding characteristics observed are the same that pure form II ($T_f$:165°C and $\Delta H_{II\text{-}F}$:120 J/g).

The presence of the N2A–H2A...O2B hydrogen bond and the π...π interaction adds cohesion in the packing of form I, possibly at the cost of twisting part of one molecule (molecule B). In form II, only the N2C–H2C...N1C hydrogen bond interaction developes, so that the N2A–H2A...O2B hydrogen bond and the π...π interaction disappear and the N2A–H2A...N1B one appears when the transition takes place. Inspecting the environment around H2A, the nearest N1B atom is found at about 4.8 Å. This way, the transition involves concomitantly the change of conformation, to yield a more planar structure, and the reorientation of the molecules.

Both crystal forms can be obtained at room temperature from different solvents. When methanol or ethanol is used, form I is obtained; on the other way, if toluene or benzene is used, form II appears. Then the solvent interactions are fundamental to decide the crystal form to be obtained.

Figures 9 and 10 show absorbance spectra for water and ethanol saturated solutions (the latter ones adequately diluted), respectively, so the total areas under the traces are a direct measure of the relative solubility between both polymorphs in each solvent. Form II was found more soluble than form I. As solubility is related to free energy, this implies that the less soluble polymorph, form I, has the lower free energy at room temperatures. In this system, conversion of form II to form I could be expected to happen at room temperature, for example via a slurry conversion experiment in suspension, but we did not observe any conversion after 24 h in water. Nevertheless, room temperature slurry conversion experiments where form II completely converts into form I have been reported by Faash et al.,[17] after much longer times (ca. 60 h) and using larger molecular concentrations (in an alcohol-water system). This confirms that form I is the more stable one, and would suggest that

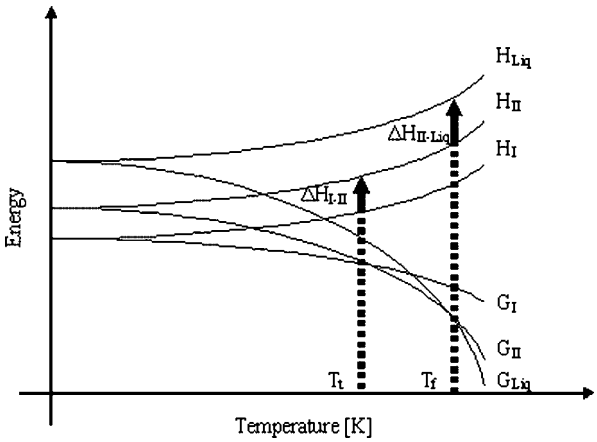


**Figure 11.** Energy versus temperature diagram of an enantiotropic dimorphic system: G, free energy; H, enthalpy; $T_t$, transition temperature; $T_f$, melting temperature.

much more that 60 h would be necessary for fully conversion in pure water.

The stability conclusion is also confirmed by the density rule,[18] which states that the crystal form with higher density is more stable at low temperature.

## CONCLUSION

The dimorphic system here described, composed by forms I and II, can be better understood in an Energy–Temperature diagram[19] as shown in Figure 11. It represents the situation for an enantiotropic system, in which form I is the stable one below the transition temperature ($T_t$), down to room temperature. At the transition temperature, ca. 127°C the free energy of form II ($G_{II}$) becomes lower than the one for form I ($G_I$) so the transition occurs and an endothermic peak is detected as a measure of the enthalpy difference between forms I and II ($\Delta H_{I\text{-}II}$). The surviving form II finally melts at around 165°C ($T_f$), when the free energy of the liquid state ($G_{Liq}$) becames lower and the corresponding enthalpy difference ($\Delta H_{II\text{-}F}$) is detected.

So form I presents a lower free energy at room temperature and should then be considered as the more stable from a thermodynamic point of view.

## ACKNOWLEDGMENTS

The provision of samples of Leflunomide by ARYL S.A. is thankfully acknowledged. The authors thank to Dr. A. Martinez, Dr. R. Baggio, and M.L. Japas for their assistance with the absorbance experiments and helpful discussions. D.V. and D.F. thank Prof J.A.K. Howard for the donation of the Rigaku AFC6S diffractometer. The Spanish Research Council (CSIC) is acknowledged for the provision of a free license of the CSD software. This work has been funded through a project of the Universidad Nacional de General San Martín.

## REFERENCES

1. Desiraju GR. 1989. Crystal engineering: the design of organic solids. New York: Elsevier.
2. Byrn SR. 1982. Solid state chemistry of drugs. New York: Academic Press.
3. Haleblian J, McCrone W. 1969. Pharmaceutical applications of polymorphism. J Pharm Sci 58:911–929.
4. Caira MR. 1998. Crystalline polymorphism of organic compounds. Top Curr Chem 198:163–208.
5. Bennett SR, Falta MT, Bill J, Kotzin BL. 2003. Antigen-specific T cells in rheumatoid arthritis. Curr Rheumatol Rep 5:255–263.
6. Calabresi P, Chabner BA. 1993. Quimioterapia de las enfermedades neoplásicas. In: Goodman-Gilman A, Rall TW, Nies AS, Taylor P, editors. Goodman and Gilman's the pharmacological basis of therapeutics, 8th edn. (Second edition of the Spanish translation). México: Editorial Médica Panamericana.
7. Breedveld FC, Dayer JM. 2000. Leflunomide: mode of action in the treatment of rheumatoid arthritis. Ann Rheum Dis 59:841–849.
8. Smolen JS, Steiner G. 2003. Therapeutic strategies for rheumatoid arthritis. Nature Rev Drug Discov 2:473–488.
9. Hansen M, Le Nours J, Johansson E, Antal T, Ullrich A, Löffler M, Larsen S. 2004. Inhibitor binding in a class 2 dihydroorotate dehydrogenase causes variations in the membrane-associated N-terminal domain. Protein Sci 13:1031–1042.
10. Olsen NJ, Stein CM. 2004. New drugs for rheumatoid arthritis. N Eng J Med 350:2167–2179.
11. Pharmacist's Drug Handbook. 2001. Johnson PH, Nale P, editors. USA: Springhouse Corporation and American Society of Health-System Pharmacists.
12. Molecular Structure Corporation. 1993. MSC/AFC Diffractometer Control Software. Version 4.3.0. Molecular Structure Corporation, 3200 Research Forest Drive, The Woodlands, TX 77381, USA.
13. Enraf-Nonius. 1994. CAD4 Express Software. Enraf-Nonius, Delft, The Netherlands, and Harms K, Wocadlo S. 1995. XCAD-4. Program for processing CAD-4 diffractometer Data. University of Marburg, Germany.
14. Sheldrick GM. 1997. SHELXS97 and SHELXL97. University of Göttingen, Germany.

15. Farrugia LJ. 1999. WinGX. J Appl Cryst 32:837–838.
16. Allen FH. 2002. The Cambridge structural database: A quarter of a million crystal structures and rising. Acta Cryst B58:380–388.
17. Faasch H, Hedtmann U, Paulus E. 2000. Crystal form of N-(4-trifluoromethylphenyl)-5-methylisoxazole-4-carboxamide. US Patent Number 6,060,494.
18. Burger A, Ramberger R. 1979. On the polymorphism of pharmaceuticals and other molecular crystals. I: theory of thermodynamic rules. Mikrochim Acta II:259–271.
19. Bernstein J. 2002. Polymorphism in Molecular Crystals. Oxford: Clarendon Press.
20. Zsolnai L, Pritzkow H. 1995. ZORTEP. An interactive ORTEP program. University of Heidelberg, Germany.